Abdominal Radiology (2019) 44:3078–3088
https://doi.org/10.1007/s00261-019-02077-1

HEPATOBILIARY

Optimal lexicon of gadoxetic acid-enhanced magnetic resonance imaging for the diagnosis of hepatocellular carcinoma modified from LI-RADS

Shin Hye Hwang[1,2,3] · Sumi Park[1] · Kyunghwa Han[2] · Jin-young Choi[2,3] · Young-Nyun Park[4] · Mi-Suk Park[2,3]

Published online: 5 June 2019
© Springer Science+Business Media, LLC, part of Springer Nature 2019

Abstract

Purpose To define the optimal lexicon of major imaging findings on gadoxetic acid-enhanced MRIs to diagnose HCC to improve diagnostic performance of the LI-RADS.

Methods Two hundred forty-one hepatic lesions (149 HCC, six other malignancies, 86 benign lesions) in 177 treatment-naïve patients at risk of HCC who underwent gadoxetic acid-MRIs from January 2013 to December 2015 were retrospectively reviewed using either histopathological or follow-up imaging findings as a standard reference. Two board-certified radiologists independently evaluated the imaging features and categorized the nodules based on the original and the following modified definitions in LI-RADS: (1) washout appearance in the portal venous phase (PVP) only versus that in the PVP or transitional phase, and (2) enhancing capsule only versus enhancing or non-enhancing capsule. Diagnostic performance and inter-observer agreement of LR-5 were assessed and compared between the algorithms using generalized estimation equation.

Results The sensitivity [79.2% (95% confidence interval 71.9, 85.0)] and accuracy [84.6% (79.5, 88.7)] of LR-5 were significantly higher for modified lexicon compared with original LI-RADS [60.4% (52.3, 67.9) and 73.9% (67.9, 79.0); $P<0.001$ in all cases]. There was no significant difference in specificity [93.5% (86.2, 97.0) and 95.7% (89.0, 98.4); $P=0.153$]. Subgroups of lesions $<$ or ≥ 2 cm showed similar tendencies. Inter-observer agreement for capsule appearance was fair to moderate, whereas that for other imaging findings was good to excellent.

Conclusions Compared to original LI-RADS, LI-RADS with modified lexicon showed higher sensitivity for the diagnosis of HCC using gadoxetic acid-MRI, with similar specificity.

Keywords Hepatocellular carcinoma · Diagnosis · MRI (Magnetic resonance imaging) · Gadoxetic acid

Introduction

Imaging plays a key role in the detection, diagnosis, and treatment planning of hepatocellular carcinoma (HCC). Most current guidelines stipulate that if strict criteria are met, a pathological confirmation is not required for the diagnosis of HCC [1–5]. Therefore, standardized terminology and reporting, as well as high quality imaging, are essential.

The Liver Imaging and Reporting and Data System (LI-RADS) was proposed in 2011 by the American College of Radiology. LI-RADS developed a comprehensive system for interpreting and reporting radiologic findings with precisely defined lexicon, which improved the clarity of radiology reports with more consistent diagnostic criteria [6]. It was originally designed for extracellular contrast media (ECCM)-enhanced dynamic imaging. And later, the use of hepatobiliary agents, gadoxetic acid and gadobenate

Electronic supplementary material The online version of this article (https://doi.org/10.1007/s00261-019-02077-1) contains supplementary material, which is available to authorized users.

✉ Mi-Suk Park
radpms@yuhs.ac

[1] Department of Radiology, National Health Insurance Service Ilsan Hospital, Goyang, South Korea

[2] Department of Radiology, Severance Hospital, Seoul, South Korea

[3] Department of Radiology, Severance Hospital, Yonsei University College of Medicine, 50-1 Yonse-ro, Seodaemun-gu, Seoul 03722, South Korea

[4] Department of Pathology, Yonsei University College of Medicine, Seoul, South Korea

dimeglumine, was incorporated into its diagnostic algorithm [7]. Unlike ECCM-enhanced magnetic resonance imaging (MRI), however, there are challenges when applying LI-RADS lexicon to gadoxetic acid-enhanced MRI. LI-RADS allows only portal venous phase (PVP) to evaluate "washout appearance" [5], and "capsule appearance" is less frequently seen in gadoxetic acid-enhanced MRIs than in ECCM-enhanced MRIs [8]. These make LI-RADS diagnostic algorithm with gadoxetic acid-enhanced MRIs yields significantly lower sensitivity than with ECCM-MRIs [8]. It undermines the key benefit of using gadoxetic acid—the higher sensitivity and earlier detection of HCC [9, 10]. To overcome it, a number of studies with small subject numbers have each made different suggestions about definition of "washout appearance" and "capsule appearance" [8, 11]. However, their combined effect has never been evaluated, whereas the controversy over their diagnostic specificity still ongoing. Therefore, a study with large population to validate variable definitions of major imaging findings proposed so far for gadoxetic acid-enhanced MRI is necessary.

The aim of this study is to suggest an optimal lexicon for major imaging findings of gadoxetic acid-enhanced MRI in the diagnosis of HCC, in order to improve the diagnostic performance of current LI-RADS.

Materials and methods

Study population

The institutional review board approved this historic cohort study and waived the requirement for informed consent. Among 3015 patients at risk of developing HCC who underwent liver dynamic MRI at our institution between January 2013 and December 2015, we included patients who were (1) treatment-naïve with risk factors for HCC (Chronic hepatitis B or liver cirrhosis of any etiology), (2) MRI using gadoxetic acid, and (3) had focal hepatic solid nodules on MRI. We limited the number and size of nodules to meet the Milan criteria. Patient with history of other malignancy within 5 years, Budd-Chiari syndrome, and whose MRI quality was not sufficient for analysis were excluded. Of these, lesions of unknown final diagnoses (treated without pathological diagnosis or followed up for less than 24 months) and malignant lesions pathologically confirmed > 180 days after the MRI were further excluded. Ultimately, 241 lesions from 177 patients were used in the analysis (Fig. 1).

Determination of final diagnosis

All hepatic malignancies were histopathologically confirmed within 180 days of the MRI. Benign lesions were diagnosed either pathologically or clinically. A senior hepatic pathologist with 25 years' experience in liver pathology carried out histopathological evaluation in accordance with the WHO Classification of Tumors of the Digestive System (2010) [12]. Histopathological sections were stained with hematoxylin–eosin and subjected to immunohistochemistry for HSP70, glutamine synthetase, glypican3, CD34, CK19, and Ki67. When histopathology was unavailable, the lesions were regarded as benign if they had disappeared or remained unchanged over a follow-up period of 24 months or longer. If a hepatic lesion presented "threshold growth" (≥ 50% diameter increase within 6 months) or imaging characteristics suggestive of malignancy during follow-up, it was excluded from the analysis. Lesions that were not followed up for a sufficient period of time were excluded from the analysis, as were those that were treated without pathological diagnosis.

Magnetic resonance imaging

All MRIs were performed using one of the following 3.0-T systems. Gadoxetic acid disodium (0.025 mmol/kg; Primovist; Bayer Pharma AG, Berlin, Germany) was administered for dynamic study. Detailed protocol for the MR acquisition is in Online Resource 1.

Image analysis

All MR images were retrospectively reviewed using a Picture Archiving and Communication System (Centricity, Version 3.0, GE Healthcare, Chicago, IL, USA). Two board-certified abdominal radiologists (S.P. and M.P., with 19 and 17 years of experience in liver MRI, respectively) independently reviewed the images. Both were blinded to the patients' clinical history or final diagnosis. The location, size, and corresponding image number of each hepatic lesion (up to five per patient, less than 5 cm in the longest diameter) were used as a guide (recorded by another investigator—study coordinator S.H.H). In each hepatic lesion, the investigators independently determined the presence or absence of major imaging features [arterial phase hyperenhancement (APHE), washout; hypoenhancement in the PVP, and enhancing capsule; enhancing rim in PVP or transitional phase (TP)] in accordance with LI-RADS version 2018 lexicon. For APHE, subtraction images in addition to arterial phase and T1-weighted images were evaluated. For modification of washout and capsule appearance, the readers evaluated the presence or absence of "TP hypointensity" and "non-enhancing capsule". A month after independent review, any discrepancies regarding the presence or absence of imaging features were resolved by consensus discussion between the two investigators. The lesion's visibility upon precedent ultrasonography, diameter, and threshold growth was recorded by the study coordinator. When available, presence of "threshold growth" was assessed using prior

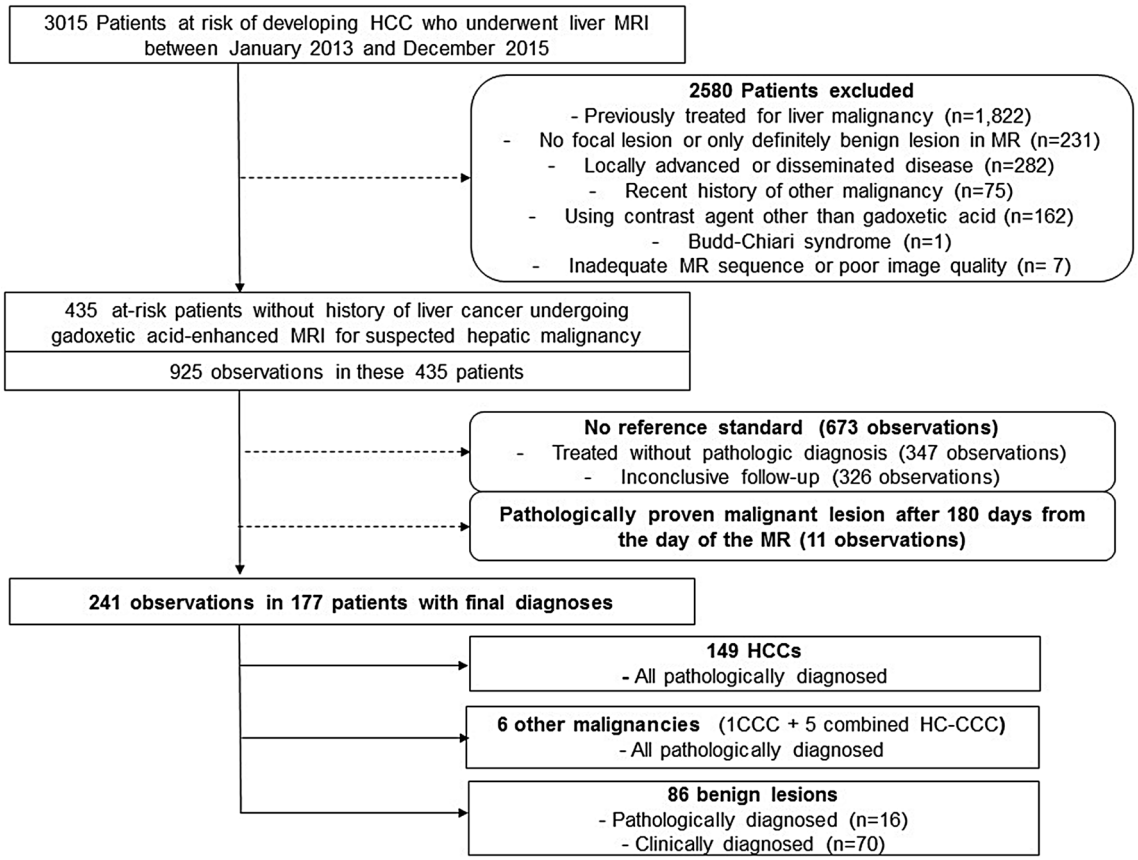

Fig. 1 Flowchart of patient selection. *MRI* magnetic resonance imaging, *HCC* hepatocellular carcinoma

cross-sectional images [MRI or computed tomography (CT)].

Afterwards, the study coordinator assigned a final category based on the original LI-RADS, LI-RADS with modified definition of washout appearance (mLI-RADSw, hypointensity in either PVP or TP), LI-RADS with modified definition of capsule appearance (mLI-RADSc, either enhancing or non-enhancing capsule), and LI-RADS with modified definition of washout and capsule appearance (mLI-RADSwc). All lesions were classified as category 3 (LR-3; indeterminate probability of malignancy), category 4 (LR-4; probably HCC), category 5 (LR-5; definitely HCC), or category M (LR-M; probably or definitely malignant but not necessarily HCC).

Statistical analysis

The sensitivity, specificity, accuracy, positive predictive value (PPV), and negative predictive value (NPV) of each algorithm for diagnosing HCC were compared with using a generalized estimating equation method with 95% confidence intervals (CIs). Subgroup analysis was also performed on the basis of lesion size: $\geq$ or <2 cm.

Inter-observer agreement regarding imaging findings and lesion category was assessed using Cohen's kappa statistics as follows: $\kappa < 0.20$, poor; 0.21–0.40, fair; 0.41–0.60, moderate; 0.61–0.80, good; and 0.81–1.00, excellent agreement [13]. All statistical analyses were performed using SPSS 23.0 (IBM, Chicago, IL, USA) and R software with the "irr" package (version 3.3.3; R Foundation for Statistical Computing, Vienna, Austria).

Results

Baseline characteristics

In our study population (177 patients; 142 men and 35 women) with median age of 58 years (range 32–80 years), hepatitis B virus infection was the most common cause of chronic liver disease [81.9% (145 of 177)]. Most of the patients [90.4% (160 of 177)] included in the study were Child–Pugh class A. Of the 241 included hepatic lesions, 149 (61.8%) were HCCs, six (2.5%) were primary hepatic malignancies other than HCC [one cholangiocarcinoma and five combined HCC-cholangiocarcinomas (cHCC-CC)],

and 86 (35.7%) were benign lesions. All hepatic malignancies were pathologically confirmed through either surgery ($n=151$) or percutaneous biopsy ($n=4$). Benign lesions were diagnosed either clinically ($n=70$) or pathologically ($n=16$; eight regenerative nodule or dysplastic nodules, five focal nodular hyperplasia-like nodules, a bile duct adenoma, a hemangioma, and a fibrocalcific nodule). An average of 1.36 lesions were included per patient. The median size of the lesions was 19.7 mm (range 2.3–48.2 mm) (Table 1).

Diagnostic performance of the LI-RADS and modified LI-RADS—for all lesions

Table 2 summarizes the diagnostic performance of original and modified lexicon of LI-RADS. Using original LI-RADS, the sensitivity, specificity, accuracy, PPV, and NPV of the category 5 for diagnosis of HCC by reviewer 1 were 58.4% (95% confidence interval 50.3, 66.0), 93.5% (95% CI 86.2, 97.0), 71.8% (95% CI 65.8–77.1), 93.5% (95% CI 86.4, 97.1), and 58.1% (95% CI 50.0, 65.8), respectively. When applying both of the modified definitions on washout and capsule appearance to the LI-RADS (mLI-RADSwc), the equivalent values were 80.5% (95% CI 73.4, 86.1), 90.2% (95% CI 82.3, 94.8), 84.2% (95% CI 79.1, 88.3), 93.0% (95% CI 87.1, 96.3), and 74.1% (95% CI 65.2, 81.4). The sensitivity, accuracy, and NPV of category 5 were significantly higher using the mLI-RADSwc (all $P<0.001$), without significant differences in specificity ($P=0.078$) or PPV ($P=0.639$) (Fig. 2).

Applying the modified definition of washout appearance (mLI-RADSw) by reviewer 1 showed the same tendency. The diagnostic sensitivity, accuracy, and NPV of the mLI-RADSw was significantly higher (all $P<0.001$), without significant differences in specificity ($P=0.078$) or PPV ($P=0.639$). When applying the modified definition of capsule appearance (mLI-RADSc) showed increased PPV ($P=0.037$) in addition to significantly higher sensitivity, accuracy, and NPV (all $P<0.001$). Specificity was not significantly different ($P>0.999$) (Table 2).

Diagnostic performance of reviewer 2 showed similar tendencies except for PPV which was not significantly changed ($P=0.077$) when applying the modified capsule appearance to LI-RADS (mLI-RADSc) (Table 2).

In consensus reading, the sensitivity, specificity, and accuracy of LR-5 in the diagnosis of HCC were 60.4% (95% CI 52.3, 67.9), 95.7% (95% CI 89.0, 98.4), and 73.9% (95% CI 67.9, 79.0) using original LI-RADS, and 79.2% (95% CI 71.9, 85.0), 93.5% (95% CI 86.2, 97.0), and 84.6% (95% CI 79.5, 88.7) using modified lexicon in LI-RADS. The sensitivity and accuracy were significantly higher for LI-RADS with modified lexicon ($P<0.001$ in all cases), without significant differences in specificity ($P=0.153$).

Table 1 Baseline characteristics of the 177 patients with 241 hepatic lesions

Characteristics	Total
Patient level	
Total number of patients	177
Age, (years); median (range)	58 (32–80)
Sex	
Male	142 (80.2%)
Female	35 (19.8%)
Cause of chronic liver disease	
Hepatitis B	145 (81.9%)
Hepatitis C	11 (6.2%)
Hepatitis B and C coinfection	3 (1.7%)
Alcohol	7 (4.0%)
Hepatitis B and alcoholics	2 (1.1%)
Unknown	9 (5.1%)
Child–Pugh class	
A	160 (90.4%)
B	17 (9.6%)
Lesion level	
Total number of lesions	241
Size (mm); median (range)	19.7 (2.3–48.2)
Final diagnosis	
Hepatocellular carcinoma	149 (61.8%)
Other malignancies	6 (2.5%)
Benign	86 (35.7%)

Diagnostic performance of the LI-RADS and modified LI-RADS—for lesions less than 2 cm

For reviewer 1, the sensitivity using LI-RADS and mLI-RADSwc was 44.0% (95% CI 31.0, 57.9) and 64.0% (95% CI 49.9, 76.0), respectively ($P<0.001$). The specificity using LI-RADS and mLI-RADSwc was 95.9% (88.0, 98.7) and 93.2% (95% CI 84.6, 97.1), respectively ($P=0.152$). For reviewer 2, the sensitivity using LI-RADS and mLI-RADSwc was 42.0% (95% CI 29.2, 55.9) and 64.0% (95% CI 49.9, 76.0), respectively ($P<0.001$). The specificity using LI-RADS and mLI-RADSwc was 97.3% (89.7, 99.3) and 94.5% (95% CI 86.3, 97.9), respectively ($P=0.152$) (Table 3).

Diagnostic performance of the LI-RADS and modified LI-RADS—for lesions between 2 and 5 cm

For reviewer 1, the sensitivity using LI-RADS and mLI-RADSwc was 65.7% (95% CI 55.8, 74.3) and 88.9% (95% CI 81.0, 93.7), respectively ($P<0.001$). The specificity using LI-RADS and mLI-RADSwc was 84.2% (95% CI 60.8, 94.8) and 78.9% (95% CI 55.4, 91.9), respectively ($P=0.304$).

Table 2 Diagnostic performance of category 5 in the diagnosis of HCC according to the original LI-RADS and mLI-RADSwc

	Reviewer 1					Reviewer 2				
	Sensitivity	Specificity	Accuracy	PPV	NPV	Sensitivity	Specificity	Accuracy	PPV	NPV
(a) LI-RADS	58.4% (50.3–66.0)	93.5% (86.2–97.0)	71.8% (65.8–77.1)	93.5% (86.4–97.1)	58.1% (50.0–65.8)	63.8% (55.7–71.1)	95.7% (89.0–98.4)	75.9% (70.1–80.9)	96.0% (89.7–98.5)	62.0% (53.7–69.6)
(b) mLI-RADSw	78.5% (71.2–84.4)	90.2% (82.3–94.8)	83.0% (77.7–87.2)	92.9% (86.8–96.2)	72.2% (63.3–79.6)	76.5% (69.0–82.6)	92.4% (84.9–96.3)	82.6% (73.7–83.9)	94.2% (88.4–97.2)	70.8% (62.1–78.3)
(c) mLI-RADSc	66.4% (58.5–73.6)	93.5% (86.2–97.0)	76.8% (71.0–81.7)	94.3% (87.9–97.4)	63.2% (54.8–70.9)	69.8% (62.0–76.6)	94.6% (87.6–97.7)	79.3% (73.7–83.9)	95.6% (89.5–98.1)	65.9% (57.4–73.5)
(d) mLI-RADSwc; (b) + (c)	80.5% (73.4–86.1)	90.2% (82.3–94.8)	84.2% (79.1–88.3)	93.0% (87.1–96.3)	74.1% (65.2–81.4)	79.9% (72.7–85.5)	92.4% (84.9–96.3)	84.6% (79.5–88.7)	94.4% (88.8–97.3	73.9% (65.1–81.1)
P-value										
(a) versus (b)	< 0.001	0.078	< 0.001	0.639	< 0.001	< 0.001	0.078	< 0.001	0.219	< 0.001
(a) versus (c)	< 0.001	> 0.999	< 0.001	0.037	< 0.001	0.002	0.315	0.010	0.545	0.005
(a) versus (d)	< 0.001	0.078	< 0.001	0.721	< 0.001	< 0.001	0.078	< 0.001	0.275	< 0.001

Numbers in parenthesis are 95% confidence intervals. Statistical significance was calculated using logistic regression analysis with generalized estimation equation

HCC hepatocellular carcinoma, *LI-RADS* Liver Imaging Reporting and Data System, *mLI-RADSw* LI-RADS with modified definition of washout appearance, *mLI-RADSc* LI-RADS with modified definition of capsule appearance, *mLI-RADSwc* LI-RADS with modified definition of washout and capsule appearance, *TP* transitional phase, *TPo* true positive, *FN* false negative, *FP* false positive, *TN* true negative, *PPV* positive predictive value, *NPV* negative predictive value

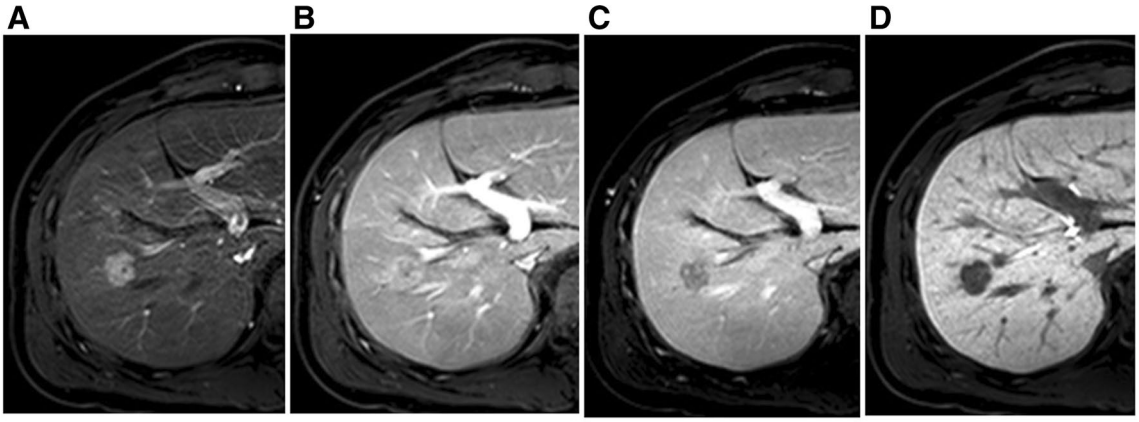

Threshold growth	Not available	US visibility	Not available
Washout on PVP	-	Washout on TP	+
Enhancing capsule	-	Nonenhancing capsule	+
LI-RADS	3	mLI-RADSwc	5

Fig. 2 A 1.8-cm HCC with Edmondson grade II–III—Category 3 on LI-RADS versus category 5 on modified LI-RADS. A 50-year-old man with hepatitis B infection had a nodule at segment 8 of the liver. There was no available antecedent surveillance ultrasonography. The lesion is hypointense compared to the surrounding parenchyma in the pre-contrast T1-weighted image (not shown), **(a)** homogenously enhanced in the arterial phase, and **(b)** remained slightly hyperintense compared to the surrounding liver in the PVP. **(c**, **d)** It becomes relatively hypointense compared to the parenchyma in the TP and hepatobiliary phase. Both readers agreed that it had a non-enhancing capsule in hepatobiliary phase. Based on the major findings of the LI-RADS, this could be a category three that may be upgraded to category 4 after considering of ancillary findings. Based on the mLI-RADSwc, it could be category 5, as confirmed using HCC on surgical pathology. *HCC* hepatocellular carcinoma, *LI-RADS* Liver Imaging Reporting and Data System, *mLI-RADSwc* LI-RADS with modified definition of washout and capsule appearance, *PVP* portal venous phase, *TP* transitional phase

Diagnostic performance of reviewer 2 showed similar tendencies (Table 4).

Inter-observer agreement among all lesions

Inter-observer agreement regarding APHE ($\kappa = 0.864$), hypointensity in the PVP ($\kappa = 0.749$), and hypointensity in the TP ($\kappa = 0.688$) were good to excellent. Agreement regarding enhancing capsules ($\kappa = 0.462$) and non-enhancing capsules ($\kappa = 0.277$) was fair to moderate.

Inter-observer agreement regarding final categorization was excellent using the LI-RADS ($\kappa = 0.879$) and the mLI-RADSwc ($\kappa = 0942$), by Cohen's kappa.

Discussion

Compared to original LI-RADS, modified lexicons in washout and capsule significantly increased sensitivity, accuracy, and NPV of gadoxetic acid-enhanced MRI without statistical change of specificity and PPV. The reported sensitivity and specificity of LI-RADS category 5 ranged from 21.1 to 72.9% and from 95.2 to 98.0%, respectively, in ECCM-enhanced MRI [14–17]. The equivalent values ranged from 72.7 to 82.6% and from 75.0 to 91.5% in in gadoxetic acid-enhanced MRI [11, 18]. Therefore, our study showed comparable sensitivity (79.9–80.5%) and specificity (90.2–92.4%) to previous ones. A few published papers reported diagnostic performance of LR-5 for lesions < 2 cm. With ECCM-enhanced MRI, LR-5 of LI-RADS v.2013.1 showed 42.3% sensitivity and 98.2% specificity [14]. With gadoxetic acid-enhanced-enhanced MRI, LR-5 of LI-RADS v.2014 showed 62.5% sensitivity and 97.7% specificity for lesions 10–19 mm in size [19]. The higher sensitivity reported by Yoon et al. than that of ours (42.0–44.0%) may be because MRI was sequentially added to CT as an additional modality in atypical cases detected in the CT.

Gadoxetic acid-MRI is not used for the purpose of determining transplant priority in the United Network for Organ Sharing (UNOS), but its uses are mostly in the regions where locoregional therapies are commonly used and early detection is aimed [4]. Therefore, customized lexicon that meets the clinical needs of such a region, namely high diagnostic sensitivity while maintaining sufficient specificity, is required. Modification of lexicon in this direction would

Table 3 Diagnostic performance of category 5 for HCC according to original LI-RADS and mLI-RADSwc; for lesions less than 2 cm

	Reviewer 1					Reviewer 2				
	Sensitivity	Specificity	Accuracy	PPV	NPV	Sensitivity	Specificity	Accuracy	PPV	NPV
(a) LI-RADS	44.0% (31.0–57.9)	95.9% (88.0–98.7)	74.8 (66.4–81.7	88.0% (68.7–96.1)	71.4% (61.7–79.5)	42.0% (29.2–55.9)	97.3% (89.7–99.3)	74.8% (66.4–81.7)	91.3% (71.1–97.8)	71.0% (61.4–79.0)
(b) mLI-RADSw	64.0% (49.9–76.0)	93.2% (84.6–97.1)	81.3% (73.4–87.2)	86.5% (71.4–94.3)	79.1% (69.2–86.4)	64.0% (49.9–76.0)	94.5% (86.3–97.9)	82.1% (74.3–87.9)	88.9% (73.9–95.8)	79.3% (69.5–86.6)
(c) mLI-RADSc	44.0% (31.0–57.9)	95.9% (88.0–98.7)	74.8 (66.4–81.7	88.0% (68.7–96.1)	71.4% (61.7–79.5)	42.0% (29.2–55.9)	97.3% (89.7–99.3)	74.8% (66.4–81.7)	91.3% (71.1–97.8)	71.0% (61.4–79.0)
(d) mLI-RADSwc; (b) + (c)	64.0% (49.9–96.0)	93.2% (84.6–97.1)	81.3% (73.4–87.2)	86.5% (71.4–94.3)	79.1% (69.2–86.4)	64.0% (49.9–76.0)	94.5% (86.3–97.9)	82.1% (74.3–87.9)	88.9% (73.9–95.8)	79.3% (69.5–86.6)
P-value										
(a) versus (b)	< 0.001	0.152	0.018	0.711	0.002	< 0.001	0.152	0.010	0.567	0.001
(a) versus (c)	> 0.999	> 0.999	> 0.999	> 0.999	> 0.999	> 0.999	> 0.999	> 0.999	> 0.999	> 0.999
(a) versus (d)	< 0.001	0.152	0.018	0.711	0.002	< 0.001	0.152	0.010	0.567	0.001

Numbers in parenthesis are 95% confidence intervals. Statistical significance was calculated using logistic regression analysis with generalized estimation equation

HCC hepatocellular carcinoma, *LI-RADS* Liver Imaging Reporting and Data System, *mLI-RADSw* LI-RADS with modified definition of washout appearance, *mLI-RADSc* LI-RADS with modified definition of capsule appearance, *mLI-RADSwc* LI-RADS with modified definition of washout and capsule appearance, *TP* transitional phase, *TPo* true positive, *FN* false negative, *FP* false positive, *TN* true negative, *PPV* positive predictive value, *NPV* negative predictive value

Table 4 Diagnostic performance of category 5 for HCC according to original LI-RADS and mLI-RADSwc; for lesions equal or larger than 2 cm

	Reviewer 1					Reviewer 2				
	Sensitivity	Specificity	Accuracy	PPV	NPV	Sensitivity	Specificity	Accuracy	PPV	NPV
(a) LI-RADS	65.7% (55.8–74.3)	84.2% (60.8–94.8)	68.6% (59.7–76.4)	95.6% (87.2–98.6)	32.0% (20.6–46.0)	74.7% (65.3–82.3)	89.5% (66.3–97.4)	77.1% (68.7–83.8)	97.4% (90.1–99.3)	40.5% (26.9–55.7)
(b) mLI-RADSw	85.9% (77.5–91.4)	78.9% (55.4–91.9)	84.7% (77.1–90.2)	95.5% (88.6–98.3)	51.7% (34.1–68.9)	82.8% (74.1–89.0)	84.2% (60.8–94.8)	83.1% (75.2–88.8)	96.5% (89.6–98.9)	48.5% (32.2–65.1)
(c) mLI-RADSc	77.8% (68.5–84.9)	84.2% (60.8–94.8)	78.8% (70.5–85.3)	96.2% (89.0–98.8)	42.1 (27.6–58.1)	83.8% (75.2–89.9)	84.2% (60.8–94.8)	83.9% (76.1–89.5)	96.5% (89.7–98.9)	50.0% (33.3–66.7)
(d) mLI-RADSwc; (b) + (c)	88.9% (81.0–93.7)	78.9% (55.4–91.9)	87.3% (80.0–92.2)	95.7% (89.0–98.4)	57.7% (38.5–74.8)	87.9% (79.9–93.0)	84.2% (60.8–94.8)	87.3% (80.0–92.2)	96.7% (90.2–98.9)	57.1% (38.7–73.8)
P-value										
(a) versus (b)	< 0.001	0.304	< 0.001	0.947	< 0.001	0.003	0.304	0.017	0.439	0.033
(a) versus (c)	< 0.001	> 0.999	< 0.001	0.109	0.002	0.002	0.304	0.009	0.457	0.019
(a) versus (d)	< 0.001	0.304	< 0.001	0.959	< 0.001	< 0.001	0.304	0.001	0.531	0.002

Numbers in parenthesis are 95% confidence intervals. Statistical significance was calculated using logistic regression analysis with generalized estimation equation

HCC hepatocellular carcinoma, *LI-RADS* Liver Imaging Reporting and Data System, *mLI-RADSw* LI-RADS with modified definition of washout appearance, *mLI-RADSc* LI-RADS with modified definition of capsule appearance, *mLI-RADSwc* LI-RADS with modified definition of washout and capsule appearance, *TP* transitional phase, *TPo* true positive, *FN* false negative, *FP* false positive, *TN* true negative, *PPV* positive predictive value, *NPV* negative predictive value

be consistent with the purpose of LI-RADS to use globally unified terms.

There is still controversy regarding the interpretation of TP hypointensity. One study reported that evaluating washout appearance in the TP of gadoxetic acid-enhanced MRI conferred significantly lower diagnostic specificity for HCC than evaluating in the PVP, although the former could increase sensitivity [20]. Hypointensity in the TP may result in "pseudo-washout", especially in hemangioma and cholangiocarcinoma [20]. In this regard, the LI-RADS stated that washout appearance should be evaluated in the PVP, not in the TP, in gadoxetic acid-enhanced MRI [7]. In our study, however, there was no case of hemangioma false positively diagnosed as a HCC due to TP pseudo-washout. Although it is challenging to diagnose hemangioma when it presents with atypical dynamic imaging pattern other than three well-known typical dynamic patterns [21], it is possible to rule out hemangiomas by means of T2-wighted sequences [22–24].

The false positive cases in our study were two pathologically proven cHCC-CCs and two clinically benign lesions (Fig. 3). Combined HCC-CCs have diverse imaging findings, reflecting the lesions' heterogeneous histology [25]. Although some radiological findings, such as rim APHE, delayed central enhancement, and peripheral washout, are thought to suggest malignancy other than HCC [26, 27], it is difficult to differentiate small cHCC-CC or hypervascular cholangiocarcinoma from HCC [28]. Moreover, prognosis has not been well established in patients with small cHCC-CC or hypervascular CCC treated in the same manner as those with HCC of equivalent-stage [29–31]. One of the false positive benign lesions progressed to an overt HCC after 32 months.

It is widely accepted that low-sensitivity imaging diagnosis of HCC, which is based on the typical hemodynamic characteristics of ECCM-enhanced MRI, primarily arises from the absence of washout appearance [32, 33]. In this regard, TP hypointensity of gadoxetic acid-enhanced MRI may be a supplementary finding that increases diagnostic sensitivity, provided that some premises are met [18]. Our study confirmed that evaluation of washout appearance in the TP did not confer significantly lower specificity than evaluation in the PVP, while it did significantly increase diagnostic sensitivity. Therefore, the concern for the specificity, based on the theoretical pharmacodynamics of gadoxetic acid, could hold less weight in practice.

Peritumoral capsule has been reported as a highly specific imaging finding in HCC (specificity 86–97%) [34–36]. However, it overlaps with washout, limiting its ability to improve diagnostic sensitivity [35]. This is an

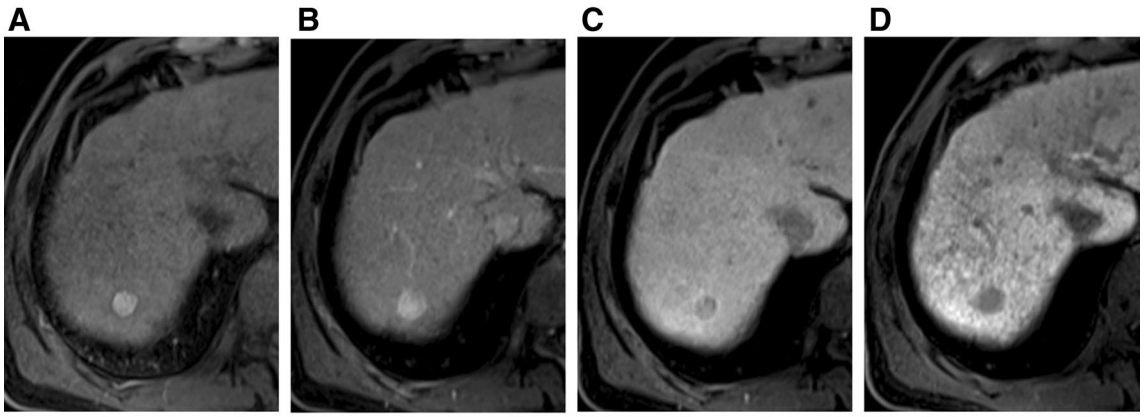

Threshold growth	No	US visibility	+
Washout on PVP	-	Washout on TP	+
Enhancing capsule	+	Nonenhancing capsule	-
LI-RADS	**4**	**mLI-RADSwc**	**5**

Fig. 3 A 1.6-cm clinically benign lesion; Category 4 in the LI-RADS versus category 5 in the mLI-RADSwc. A 66-year-old man with alcoholic liver disease had a nodule at segment 7 of the liver. The lesion was hyperintense compared to the surrounding parenchyma in the pre-contrast T1-weighted image and **(a**, **b)** an APHE lesion remained hyperintense with the adjacent parenchyma in the PVP. **c**, **d** In the TP and hepatobiliary phase, it was a hypointense lesion. Both observers agreed that there was an enhancing capsule. It was category 4 according to the LI-RADS algorithm and category 5 according to mLI-RADSwc. LI-RADS, Liver Imaging Reporting and Data System; mLI-RADSwc, LI-RADS with modified definition of washout and capsule appearance; *APHE* arterial phase hyperenhancement, *PVP* portal venous phase, *TP* transitional phase

even greater problem in gadoxetic acid-enhanced MRI, because strong enhancement of the hepatic parenchyma in the TP, caused by hepatocytic uptake of contrast media, may obscure enhancing capsule appearance and thus reduce diagnostic sensitivity [37]. A recent radiologic-pathologic correlation study reported that the presence of a smooth, dark, non-enhancing rim in the hepatobiliary phase was better correlated with the presence of histological capsule than was conventional enhancing capsule appearance [11]. Our study showed that adding non-enhancing rim to the conventional enhancing capsule appearance as a major feature significantly increased sensitivity without change in specificity.

With regards to capsule appearance, low inter-observer agreement may be more of a problem than diagnostic performance [38–41]. In the present study, inter-observer agreement regarding conventional enhancing capsule appearance was moderate. Agreement regarding non-enhancing capsule was only fair, even though the two reviewers were experts in gadoxetic acid-enhanced MRI and had similar levels of experience. On the other hand, the inter-observer agreement regarding washout appearance was good in both the PVP and TP in the present study.

The major limitation of this study was its retrospective design, which may have resulted in selection bias. To minimize this, we defined strict inclusion and exclusion criteria in a representative historic cohort. Secondly, most of the benign lesions [81.4% (70 of 86)] in the present study were not histopathologically confirmed. To minimize over- or underestimation of the diagnostic performance for HCC, we excluded radiologically definite cysts and shunts. In addition, considering the previously reported doubling time of HCC, we only included clinically benign lesions that had been followed up for more than 2 years [42]. If only histopathologically confirmed benign lesions had been taken into account, it would not reflect actual clinical practice. In addition, any lesions thought to have become malignant during follow-up were removed from the study to exclude interval cancers. Thirdly, we focused on LR-5, which was based solely on major imaging features. Therefore, we could not evaluate diagnostic performance of LI-RADS categories when applying the ancillary features.

In conclusion, the modified lexicon regarding the definition of washout and capsule appearance in gadoxetic acid-enhanced MRI showed higher sensitivity than the original LI-RADS diagnostic algorithm for hepatobiliary agents, while maintaining specificity, in the diagnosis of HCC.

Funding All authors declare that they have nothing to disclose about funding with respect to this manuscript.

Compliance with ethical standards

Conflict of interest The authors of this study declared that they have nothing to disclose regarding conflict of interest with respect to this manuscript.

Ethical approval All procedures performed in studies involving human participants were in accordance with the ethical standards of the institutional and/or national research committee and with the 1964 Helsinki Declaration and its later amendments or comparable ethical standards.

References

1. (2012) EASL-EORTC clinical practice guidelines: management of hepatocellular carcinoma. J Hepatol 56(4):908-943.
2. Kudo M, Matsui O, Izumi N, Iijima H, Kadoya M, Imai Y (2014) Surveillance and diagnostic algorithm for hepatocellular carcinoma proposed by the Liver Cancer Study Group of Japan: 2014 update. Oncology 87 Suppl 1:7-21.
3. Bruix J, Sherman M (2011) Management of hepatocellular carcinoma: an update. Hepatology 53(3):1020-1022.
4. Korean Liver Cancer Study Group, National Cancer Center, Korea (2015) 2014 Korean Liver Cancer Study Group-National Cancer Center Korea practice guideline for the management of hepatocellular carcinoma. Korean J Radiol 16(3):465-522.
5. Mitchell DG, Bruix J, Sherman M, Sirlin CB (2015) LI-RADS (Liver Imaging Reporting and Data System): summary, discussion, and consensus of the LI-RADS Management Working Group and future directions. Hepatology 61(3):1056-1065.
6. Lee VS (2017) Annual Oration: Driving Value through Imaging. Radiology 285(1):3-11.
7. Hope TA, Fowler KJ, Sirlin CB, Costa EA, Yee J, Yeh BM, Heiken JP (2015) Hepatobiliary agents and their role in LI-RADS. Abdom Imaging 40(3):613-625.
8. Song JS, Choi EJ, Hwang SB, Hwang HP, Choi H (2018) LI-RADS v2014 categorization of hepatocellular carcinoma: Intraindividual comparison between gadopentetate dimeglumine-enhanced MRI and gadoxetic acid-enhanced MRI. Eur Radiol https://doi.org/10.1007/s00330-018-5559-z.
9. Lee YJ, Lee JM, Lee JS, Lee HY, Park BH, Kim YH, Han JK, Choi BI (2015) Hepatocellular carcinoma: diagnostic performance of multidetector CT and MR imaging-a systematic review and meta-analysis. Radiology 275(1):97-109.
10. Kierans AS, Kang SK, Rosenkrantz AB (2016) The Diagnostic Performance of Dynamic Contrast-enhanced MR Imaging for Detection of Small Hepatocellular Carcinoma Measuring Up to 2 cm: A Meta-Analysis. Radiology 278(1):82-94.
11. An C, Rhee H, Han K, Choi JY, Park YN, Park MS, Kim MJ, Park S (2017) Added value of smooth hypointense rim in the hepatobiliary phase of gadoxetic acid-enhanced MRI in identifying tumour capsule and diagnosing hepatocellular carcinoma. Eur Radiol 27(6):2610-2618.
12. Theise ND CM, Franceschi S (2010) Hepatocellular carcinoma. In: Bosman FT CF, Hruban RH, Theise ND (ed) WHO classification of tumours of the digestive system. Lyon: International agency of research on cancer, pp 205-216.
13. Landis JR, Koch GG (1977) The measurement of observer agreement for categorical data. Biometrics 33(1):159-174.
14. Darnell A, Forner A, Rimola J, Reig M, Garcia-Criado A, Ayuso C, Bruix J (2015) Liver Imaging Reporting and Data System with MR Imaging: Evaluation in Nodules 20 mm or Smaller Detected in Cirrhosis at Screening US. Radiology 275(3):698-707.

15. Zhang YD, Zhu FP, Xu X, Wang Q, Wu CJ, Liu XS, Shi HB (2016) Liver Imaging Reporting and Data System:: Substantial Discordance Between CT and MR for Imaging Classification of Hepatic Nodules. Acad Radiol 23(3):344-352.
16. Becker AS, Barth BK, Marquez PH, Donati OF, Ulbrich EJ, Karlo C, Reiner CS, Fischer MA (2017) Increased interreader agreement in diagnosis of hepatocellular carcinoma using an adapted LI-RADS algorithm. Eur J Radiol 86:33-40.
17. Lee SE, An C, Hwang SH, Choi JY, Han K, Kim MJ (2018) Extracellular contrast agent-enhanced MRI: 15-min delayed phase may improve the diagnostic performance for hepatocellular carcinoma in patients with chronic liver disease. Eur Radiol 28(4):1551-1559.
18. Cha DI, Jang KM, Kim SH, Kang TW, Song KD (2017) Liver Imaging Reporting and Data System on CT and gadoxetic acid-enhanced MRI with diffusion-weighted imaging. Eur Radiol 27(10):4394-4405.
19. Yoon JH, Lee JM, Lee YJ, Lee KB, Han JK (2019) Added Value of sequentially performed gadoxetic acid-enhanced liver MRI for the diagnosis of small (10-19 mm) or atypical hepatic observations at contrast-enhanced CT: A prospective comparison. J Magn Reson Imaging 49(2):574-587.
20. Joo I, Lee JM, Lee DH, Jeon JH, Han JK, Choi BI (2015) Noninvasive diagnosis of hepatocellular carcinoma on gadoxetic acid-enhanced MRI: can hypointensity on the hepatobiliary phase be used as an alternative to washout? Eur Radiol 25(10):2859-2868.
21. Vilgrain V, Boulos L, Vullierme MP, Denys A, Terris B, Menu Y (2000) Imaging of atypical hemangiomas of the liver with pathologic correlation. Radiographics 20(2):379-397.
22. McFarland EG, Mayo-Smith WW, Saini S, Hahn PF, Goldberg MA, Lee MJ (1994) Hepatic hemangiomas and malignant tumors: improved differentiation with heavily T2-weighted conventional spin-echo MR imaging. Radiology 193(1):43-47.
23. Soyer P, Dufresne AC, Somveille E, Scherrer A (1997) Hepatic cavernous hemangioma: appearance on T2-weighted fast spin-echo MR imaging with and without fat suppression. AJR Am J Roentgenol 168(2):461-465.
24. Bennett GL, Petersein A, Mayo-Smith WW, Hahn PF, Schima W, Saini S (2000) Addition of gadolinium chelates to heavily T2-weighted MR imaging: limited role in differentiating hepatic hemangiomas from metastases. AJR Am J Roentgenol 174(2):477-485.
25. Park SH, Lee SS, Yu E, Kang HJ, Park Y, Kim SY, Lee SJ, Shin YM, Lee MG (2017) Combined hepatocellular-cholangiocarcinoma: Gadoxetic acid-enhanced MRI findings correlated with pathologic features and prognosis. J Magn Reson Imaging 46(1):267-280.
26. Fowler KJ, Potretzke TA, Hope TA, Costa EA, Wilson SR (2018) LI-RADS M (LR-M): definite or probable malignancy, not specific for hepatocellular carcinoma. Abdom Radiol (NY) 43(1):149-157.
27. Horvat N, Nikolovski I, Long N, et al. (2018) Imaging features of hepatocellular carcinoma compared to intrahepatic cholangiocarcinoma and combined tumor on MRI using liver imaging and data system (LI-RADS) version 2014. Abdom Radiol (NY) 43(1):169-178.
28. Fowler KJ, Sheybani A, Parker RA, 3rd, Doherty S, E MB, Chapman WC, Menias CO (2013) Combined hepatocellular and cholangiocarcinoma (biphenotypic) tumors: imaging features and diagnostic accuracy of contrast-enhanced CT and MRI. AJR Am J Roentgenol 201(2):332-339.
29. Korean Society of Abdominal R (2017) Diagnosis of Hepatocellular Carcinoma with Gadoxetic Acid-Enhanced MRI: 2016 Consensus Recommendations of the Korean Society of Abdominal Radiology. Korean J Radiol 18(3):427-443.
30. Kim JH, Won HJ, Shin YM, Kim KA, Kim PN (2011) Radiofrequency ablation for the treatment of primary intrahepatic cholangiocarcinoma. AJR Am J Roentgenol 196(2):W205-209.
31. Takahashi K, Obeid J, Burmeister CS, Bruno DA, Kazimi MM, Yoshida A, Abouljoud MS, Schnickel GT (2016) Intrahepatic Cholangiocarcinoma in the Liver Explant After Liver Transplantation: Histological Differentiation and Prognosis. Ann Transplant 21:208-215.
32. Forner A, Vilana R, Ayuso C, et al. (2008) Diagnosis of hepatic nodules 20 mm or smaller in cirrhosis: Prospective validation of the noninvasive diagnostic criteria for hepatocellular carcinoma. Hepatology 47(1):97-104.
33. Park MS, Kim S, Patel J, Hajdu CH, Do RK, Mannelli L, Babb JS, Taouli B (2012) Hepatocellular carcinoma: detection with diffusion-weighted versus contrast-enhanced magnetic resonance imaging in pretransplant patients. Hepatology 56(1):140-148.
34. Khan AS, Hussain HK, Johnson TD, Weadock WJ, Pelletier SJ, Marrero JA (2010) Value of delayed hypointensity and delayed enhancing rim in magnetic resonance imaging diagnosis of small hepatocellular carcinoma in the cirrhotic liver. J Magn Reson Imaging 32(2):360-366.
35. Rimola J, Forner A, Tremosini S, Reig M, Vilana R, Bianchi L, Rodriguez-Lope C, Sole M, Ayuso C, Bruix J (2012) Non-invasive diagnosis of hepatocellular carcinoma </= 2 cm in cirrhosis. Diagnostic accuracy assessing fat, capsule and signal intensity at dynamic MRI. J Hepatol 56(6):1317-1323.
36. Choi SH, Byun JH, Lim YS, Yu E, Lee SJ, Kim SY, Won HJ, Shin YM, Kim PN (2016) Diagnostic criteria for hepatocellular carcinoma 3 cm with hepatocyte-specific contrast-enhanced magnetic resonance imaging. J Hepatol 64(5):1099-1107.
37. Cho ES, Choi JY (2015) MRI features of hepatocellular carcinoma related to biologic behavior. Korean J Radiol 16(3):449-464.
38. Fowler KJ, Tang A, Santillan C, et al. (2018) Interreader Reliability of LI-RADS Version 2014 Algorithm and Imaging Features for Diagnosis of Hepatocellular Carcinoma: A Large International Multireader Study. Radiology 286(1):173-185.
39. Chernyak V, Flusberg M, Law A, Kobi M, Paroder V, Rozenblit AM (2018) Liver Imaging Reporting and Data System: Discordance Between Computed Tomography and Gadoxetate-Enhanced Magnetic Resonance Imaging for Detection of Hepatocellular Carcinoma Major Features. J Comput Assist Tomogr 42(1):155-161.
40. Ehman EC, Behr SC, Umetsu SE, Fidelman N, Yeh BM, Ferrell LD, Hope TA (2016) Rate of observation and inter-observer agreement for LI-RADS major features at CT and MRI in 184 pathology proven hepatocellular carcinomas. Abdom Radiol (NY) 41(5):963-969.
41. Zhang YD, Zhu FP, Xu X, Wang Q, Wu CJ, Liu XS, Shi HB (2016) Classifying CT/MR findings in patients with suspicion of hepatocellular carcinoma: Comparison of liver imaging reporting and data system and criteria-free Likert scale reporting models. J Magn Reson Imaging 43(2):373-383.
42. An C, Choi YA, Choi D, Paik YH, Ahn SH, Kim MJ, Paik SW, Han KH, Park MS (2015) Growth rate of early-stage hepatocellular carcinoma in patients with chronic liver disease. Clin Mol Hepatol 21(3):279-286.

Publisher's Note Springer Nature remains neutral with regard to jurisdictional claims in published maps and institutional affiliations.